PROCEEDINGS OF THE INTERNATIONAL CONFERENCE
NANOMATERIALS: APPLICATIONS AND PROPERTIES
Vol. **2**No 2, 02PCN29(6pp) (2013)

Low-temperature Sol-gel Approach for Creating New Functional Nanomaterials

A.V. Vinogradov*, V.V.Vinogradov†

Institute of Solution Chemistry of Russian Academy of Science, 1, Akademicheskaya str., 153045 Ivanovo, Russia

(Received 10 Juny 2013; published online 02 September 2013)

It is well-known that production of a crystal matrix is as a rule accompanied by using high-temperature processing which considerably limits the area of applied use of the objects. In the present work, we consider new approaches aimed at formation of crystalline highly active oxide phases without using annealing stage by achieving deep intercomponent penetration of disperse particles at the nanolevel during the sol-gel process reactions. The use of these approaches was possible in a single stage for the first time: 1) entrapment of various biological objects in a ceramic biocompatible matrix necessary for obtaining vaccines of new generation; 2) doping a crystal lattice up to 10at. % usingsoft chemistry method; 3) chemical modification of biopolymers for the purpose of developing high-level operational characteristics. In this work, trends in forming crystals from solutions for existing ceramic matrices are analyzed for the first time. The main objects of study are materials of modified titania and alumina.

Keywords: Low-temperature sol-gel, titania, alumina, thermal stability, photoactivity, biomaterials.

PACS numbers: 61.05.C

1. WHAT DOES «LOW-TEMPERATURE SOL-GEL» MEAN?

The traditional technology of the sol-gel method consists in synthesizing materials, including nanomaterials, which involves obtaining a sol with a subsequent transformation of that into a gel, in which solvent molecules are caged in a flexible, but fairly steady three-dimensional grid formed by hydroxide particles. As a result, most materials obtained using this classical method require post-processing for the purpose of transforming amorphous hydroxide particles into crystalline state. Using titania and alumina (the most popular objects) as an example is especially topical, since the amorphous phase does not exhibit catalytic activity. In our recentpapers, following last trends in the area of inorganic materials technology, we have shown that in neutral aqueous solutions it is possibleto produce inorganic polymers generated from nanocrystalline sol. The amorphous phase contenttherefore does not exceed 5 %, and activity of obtained samples is comparable to that of calcined ones. Thus, approaches aimedatdeveloping single-phaseprocesses of polycondensation for crystalline products of hydrolysis of molecular precursors to form an ordered ceramic array can be classified as "Low-temperature sol-gel".

2. SYNTHESIS AND THERMAL STABILITY OF BIOMATERIALS ALBUMINS@ALUMINA

Three proteins of the albumins family were selected for that study: Ovalbumin (OVA), bovine serum albumin (BSA) and human serum albumin (HSA). Various entrapment procedures were used, denoted I-IV. In what follows we use the following notation: protein@alumina-method (e.g., BSA@alumina-IV), where protein is OVA, BSA or HSA, and methods are (as detailed in the Experimental Details): I - catalysis with NaF, II – peptization with acetic acid, III - peptization with nitic acid, and IV - ultrasonic preparation at neutral pH, which is the main novel procedure of this report. It should be noted that the use of acetic acid and particularly of ultrasonic treatment provide solution pH values of 4.8 and 7.3, respectively, that are comfortable for biomolecules and corresponds to an optimum range at which the albumin molecules

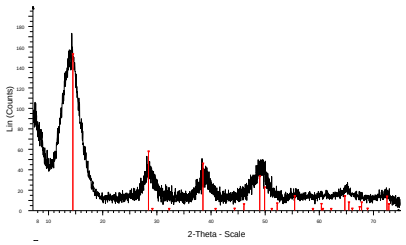

Fig. 1 - XRD diffractogram of OVA@alumina-I. (The red lines are the literature XRD peaks for Boehmite (JCPDS file No. 21-1307)

and the particles have opposite charges, providing the needed electrostatic interaction for entrapment.

One should first be sure that the proteins were entrapped at all. The thermal behavior is a strong indicator, and we return to it below in the context of the improved thermal stability of the dopant.

It is important to determine the type of the alumina synthesized. Of the six crystalline phases of alumina the biologically active form of alumina used as an adjuvant in current vaccines is boehmite/pseudoboehmite. XRD analyses of all of the aluminas indicated typical boehmite structure, Fig. 1., and Scherer-equation analysis provides an elementary crystallite size of few nm (typically 3-4 nm).

AFM pictures in the semi-contact mode of the dried samples reveal the aggregation of these elementary particles into larger particles of several tens of nm, as shown for instance for HSA@alumina-II (Fig. 2).

*vav@isc-ras.ru
†vvv@isc-ras.ru

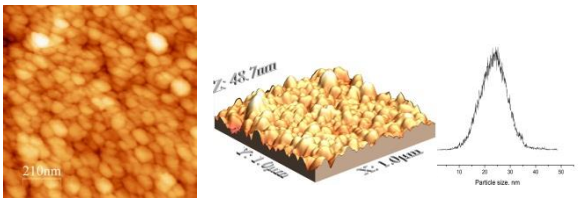

a *b* *c*

Fig. 2 - Two (a) and three – dimensional (b) AFM images of the HSA@alumina-II and its particle size distribution (c).

Surface area and porosity analyses (by nitrogen adsorption, analyzed by the BET and BJH equations) conformed with typical microporosity, with some induced changes due to the protein entrapment. For instance, for the most promising method for bio-applications – the ultrasonic method – the values before protein entrapment were: surface area of 246 m^2/gr, pore volume of 0.23 cm^3/gr and pore size of ~ 4 nm, with an increase, after entrapment, to 370 and 356 m^2/gr for BSA and HSA, respectively, an increase to 0.34 cm^3/gr for both proteins , and with little change in the average pore size. It seems that the effect of the protein is to interfere with the aggregation, resulting in a more open structure.

The thermal stability of proteins is a very strict limitation of their use for various medical and industrial applications, often requiring refrigeration. It is for that reason that the observation of enhanced stability of enzymes in sol-gel matrices has led to numerous studies of this effect [1-4]. The vast majority (if not all) of the stability studies have been carried out within silica sol-gel matrices, and we could not locate similar studies in sol-gel alumina matrices. As explained above, the injectability of alumina makes this potential stabilization even more relevant and interesting. Another novelty of this study is that the stability studies have been carried out by a method, which to the best of our knowledge has not been used so far in studies of sol-gel entrapped protein stability, namely differential scanning calorimetry (DSC). DSC has been traditionally used for the follow-up of phase transitions of within materials, but less known is the use of DSC to determine phase transitions in proteins which are due to the denaturation process. Indeed, proteins demonstrate a DSC peak (either the original curve or its second derivative – we use both below) upon that heating process. This is also observed for adsorbed proteins, which in any event decreases the denaturation temperature. As seen in Fig. 3, the denaturation temperature of OVA is shifted by 30 degrees when entrapped by method I after three days of aging and reaches 100 °C, an extremely high temperature for denaturation.

Similar stabilization was observed for BSA@alumina-II and III (Fig. 4 left). An exceptionally high stabilization was obtained for HSA in HSA@alumina-IV: An increase of 54 °C to a denaturation temperature of 120 °C (!) (Fig. 4 right), highlighting the ultrasonic sol-treatment without acids as a method of choice for proteins.

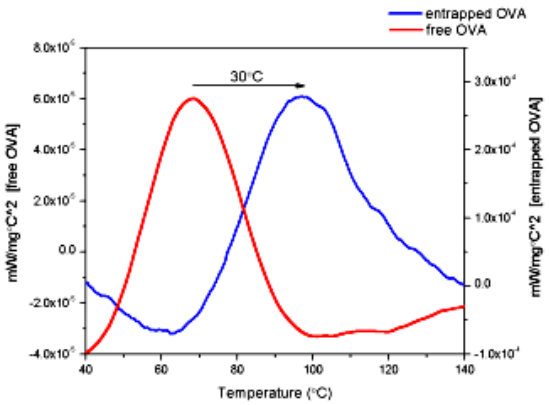

Fig. 3 - DSC analysis: A increase of 30 °C in the denaturation temperature to 100 °C is observed for OVA@alumina-I (right curve), compared with free OVA (left curve).

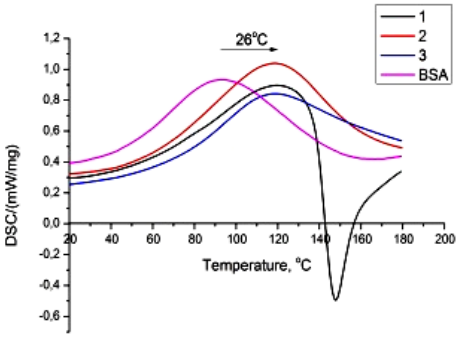

a

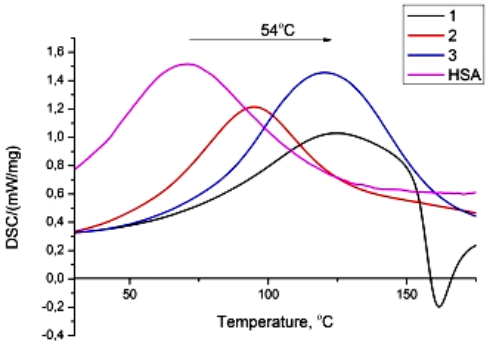

b

Fig. 4 - DSC analyses of free and entrapped BSA(a) and free and entrapped HSA(b): 1-protein@alumina-III, 2-protein@alumina-II, 3-protein@alumina-IV.

So, in this part of application of Low-temperature sol-gel approach we have developed methods for the unharmful entrapment in alumina, showed that DSC can serve as a sensitive tool for the analysis of thermal stability of entrapped proteins, found by this method marked stabilization of the entrapped proteins in alumina, and thus believe have opened a potential door for sol-gel materials to be considered as injectable carriers of bioactive molecules. Animal studies on the immunogenic activity and release of OVA from OVA@alumina (OVA is a common model for vaccination studies), as well as further activity and stability studies on additional proteins will be reported in due course.

3. A SIMPLE PREPARATION OF HIGHLY PHOTOACTIVE TITANIADOPED NANOCRYSTALS

Nanoscaled Fe(III)-doped TiO_2 crystalline particles, which exhibited high photocatalytic activity and excellent photoelectrochemical properties under visible light irradiation, were successfully synthesized by low-temperature sol-gel formation of titania sol in the presence of magnetite phase without annealing for the first time.

In this work, we have both shown the possibility of obtaining highly photoactive TiO_2 nanoparticles without annealing and carried out doping the anatase crystal lattice by the Fe^{3+} ions up to 13at.% in a single-phase crystal formation.

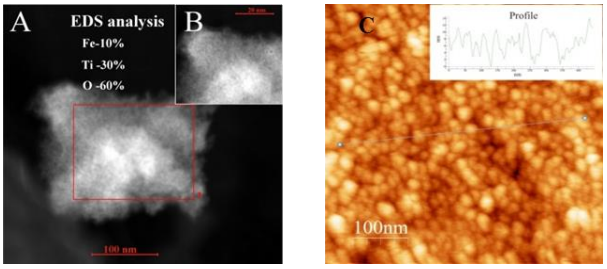

Fig. 1 - Morphology of as-prepared Fe(III)-doped TiO_2 nanoproducts by (A, B) STEM and (C) AFM analysis. EDS analysis of nanoproducts recorded from the red frame in (A).

Doping nanoparticles in an aqueous solution was performed during the process of intercomponental penetration of disperse phases at the nanolevel in the multiphase colloidal system, in which the magnetite sol particles were used as crystallization centers for the products of titanium tetraisopropylate hydrolysis. Heating to 80°C promoted the processes of thermal dehydration and an increase in crystallinity of nanoparticles. The obtained Fe(III)-doped TiO_2 nanoparticles exhibited high photocatalytic activity and excellent photoelectrochemical properties under visible light irradiation. Fig. 1 shows the typical AFM and SEM images of the as-prepared Fe(III)-doped TiO_2 nanoproducts.

It can be seen that the Fe-TiO_2 nanoproducts are uniform and have an average size of formations of about 10 nm (see. Fig. 1 C profile). A detailed analysis of morphology of particles of the Fe-TiO_2 powder (dried in the air at 80°C) according to STEM, Fig.1A shows the formation of highly porous aggregates produced from nanoparticles with narrow size distribution. According high-resolution transmission electron micrograph (HRTEM), Fig.2, it is found that the material represents a single-phase system containing 7-13 at.% of Fe(III)-TiO_2. Fig. 2 (A,C) shows HRTEM images of the Fe-TiO_2 nanoparticles. The morphology of Fe_3O_4 crystalline nanoparticles investigated by HRTEM is represented on Fig. 2 (D,G).

The structure of the particles is characterized by clear crystalline lattice fringes, with an average size of crystalline formations of about 5 nm, Fig. 2C,which correspond to the (101) planes of the body-centered tetragonal structure of anatase.

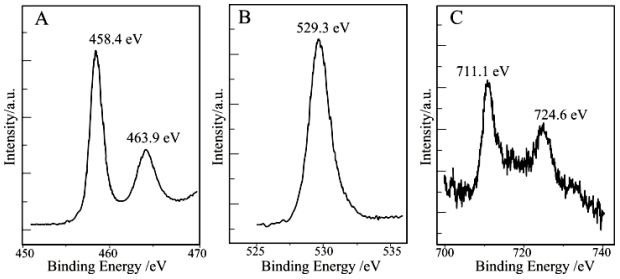

Fig. 2 - HRTEM images(A,B) of as-prepared Fe(III)-doped TiO_2 nanoproducts and HRTEM images (D,C) of as-prepared Fe_3O_4 nanoparticles: (A,D) low magnification image; (B,F) the SAED pattern recorded from the A,D-image ; (C,G) high magnification image.

The attached SAED pattern (shown in Fig. 2B,) could be indexed as the (101) zone axis diffraction[5], which further confirmed the single crystalline anatase structure. The nanocrystallization of the TiO_2 doped framework is very important for applying it in devices utilizing its semiconductor properties, such as photocatalysis and solar energy conversion. The HRTEM images confirm that the process of interface interaction of products of titanium isopropylate hydrolysis using magnetite phase particles as crystallization centers leads to formation of a single-phase ultradisperse material which possesses a high degree of crystallinity.

An assessment of the surface chemical composition and electronic state of the Fe-TiO_2 crystallites is archived by using XPS (Fig. 3). Ti 2p and O 1s show their characteristic peaks (458.4 eV and 463.9 eV for Ti2p, 529.3 eV for O1s), typical binding energies for Ti^{4+} and O^{2-} in TiO_2[6].

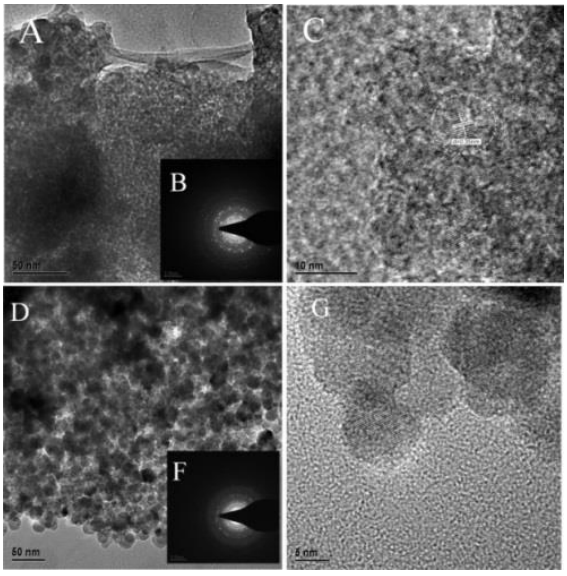

Fig. 3 – The XPS spectrum of the 10 at% Fe(III)/TiO_2 focusing of Ti 2p, O 1s, and Fe 2p peaks.

The XPS confirms the presence of Fe species with two relatively weak binding energy peaks of 711.1eV and 724.6 eV, corresponding to Fe(III). Note that the binding energies of Fe^{3+} exhibits a positive shift when compared to those in Fe_2O_3 (710.7 eV for 2p3/2 and 724.2 eV for 2p1/2), which is due to the Fe–Ti interaction. The absence of ironoxyhydroxide phase is related with high

crystallinity of magnetite phase fig.2(F,G).

Apparently, in this case doping the titania crystal lattice by the Fe^{3+} ion occurs at the stage of crystallization of titanium isopropylate hydrolysis products. This is due to the magnetite phase decomposition [7] in a highly acidic aqueous solution according to the following transformation scheme:

$$Fe_3O_4+H_2O+H^+ \rightarrow [FeO(OH)]_2(FeOH) \rightarrow 2FeO(OH)+FeOH^+$$

Thus, magnetite, while in a highly acidic medium, turns into a state of unstable hydroxo complexes which form the $FeOH^+$ ions and Fe(III) oxide monohydrate in an aqueous solution. Thus formed FeO(OH) nanocrystallites act as crystallization centers for titania formed in the process of titanium isopropylate hydrolysis, since they have identical crystal systems (tetragonal) and ionic radii of cations.

The photocatalytic activities of Fe(III)-doped TiO_2 samples containing different amount of iron and pure TiO_2 were evaluated in terms of the decolorization of Rhodamine B (RB) dye under visible light, as shown in Fig. 4(A). According to Fig. 4A, RB can be almost completely decolorized within 2 h on 10 at.% Fe(III)-doped TiO_2, whereas for the pure TiO_2 the decolorization rate of RB was significantly lower (50%) than that of the Fe(III)-doped TiO_2 at the same period. It was found that the most pronounced photocatalytic effect is attained upon doping the anatase crystal lattice by more than 7 at.% and less than 13 at.% of iron. It has been shown that excessive dopants can act as recombination centers, promoting the recombination of electron-hole pairs and increasing semiconductor properties. At the same time, activity of the synthesized species is similar to that of calcined titania-based materials [8-9]. The reason for that is the formation of a highly porous structure which collapses by annealing. The specific surface area of the synthesized products for Fe(III)-doped powders and pure TiO_2 has appeared to be virtually identical and amounted to about 160 m^2/g). Besides, the obtained nanoparticles possess a high degree of crystallinity that corresponds to high semiconductor characteristics and leads to an increase in photocatalytic activity. These results imply high potential application in the utilization of solar light, the absence of a stage of annealing for preserving functional characteristics of materials allowing to coat a photocatalytically active layer of the Fe-TiO_2 nanoparticles on finished surfaces, including those possessing low thermal stability. The photocurrent response measurement was carried out under visible light irradiation to investigate the photo-induced charge separation efficiency of Fe(III)-doped TiO_2 samples containing different amount of iron and pure TiO_2.

As shown in Fig. 4(B), the photocurrent of 10% Fe-TiO_2 (54μA/cm^2) is 3.6 times as much as that of non-modified TiO_2 (15 μA/cm^2), which indicates that Fe-TiO_2 has higher separation efficiency of the photo-induced charges than non-modified TiO_2.

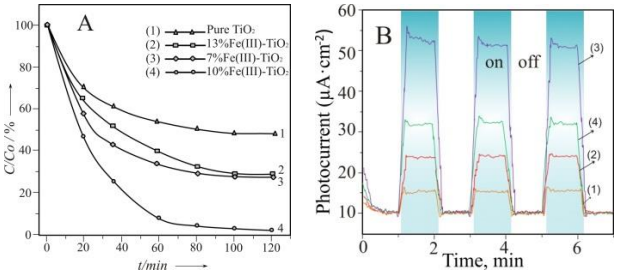

Fig. 4 - Photocatalytic activities (A) and photocurrent responses (B) of Fe(III)-doped TiO_2 samples containing different amounts of iron: ((2) 13 at.% Fe(III); (3) 7 at.% Fe(III); (4) 10 at.% Fe(III)) and pure TiO_2 (1) under visible light.

It is understood that in the as-prepared Fe-TiO_2 the photo-induced electrons are transferred from the semiconductor surface to the counter electrode via an external circuit under visible light illumination. Recently, Ren Su et al. [9] reported a high-quality Fe-doped TiO_2 films with superior visible-light performance via one-step electrochemical oxidation. Accordingly the photovoltaic test our films demonstrate an excellent superiority, even the annealing free. The photocatalytic activity of a catalyst greatly depends on the electron-hole transfer ability.So, a change in photocatalytic activity of Fe(III) doped-TiO_2 with altering the at.% iron content is in good agreement with its charge transfer.

In conclusion, we have successfully performed a synthesis by low-temperature sol-gel formation of titania sol in the presence of magnetite phase without annealing for the first time. As a result, highly porous nanoparticles with clear crystalline lattice fringes were obtained. These products possess high potential application in the utilization of solar light. The absence of a stage of annealing while forming the titania photoactive nanoparticles active in the visible solar light region opens wide prospects of practical use and creating functional films in situ. In particular, there is a possibility of coating photoactive layers of the Fe-TiO_2 nanoparticles on finished surfaces, including those possessing low thermal stability.

4. NEW APPROACH TO APPLY CRYSTALLINE TITANIA HYDROSOLS ON THE COTTON CLOTH

Crystalline titania hydrosols have been used to treat cotton fibers. 1,2,3,4-Butanetetracarboxylic acid was applied as a cross-linking agent. Self-cleaning effect of the textile materials modified with titania nanoparticles was evaluated using the reaction of Rhodamine B decomposition under UV radiation in water media. Despite high photocatalytic characteristics of processed cotton fibers, mechanical properties strongly depend on the type of applied acid used for peptization of titania. It is shown that the use of strong acids as titania hydrosol components results in cellulose glycosidic bond cleavage and a sharp decrease in mechanical durability of a cotton fiber. Modified cotton fibers exhibit high self-cleaning properties retained even after five washing cycles.

Scanning electronimages of modified cotton fibers

For studying the morphology of the obtained materials, scanning electron images of non-processed (*Fig. 1A–B)* and processed TiO_2 textile fibers (*Fig. 1C–D)*

have been taken. Processing cotton fibers by crystalline titania hydrosol obviously does not result in formation of large-scale aggregates on their surface (*Fig. 1C-D*), accordingly with the earlier results [10], but, on the contrary, allows to reach uniform distribution along the entire surface due to high sedimentation stability of the sol (more than 2 months) and small size of particles (Fig. 2).

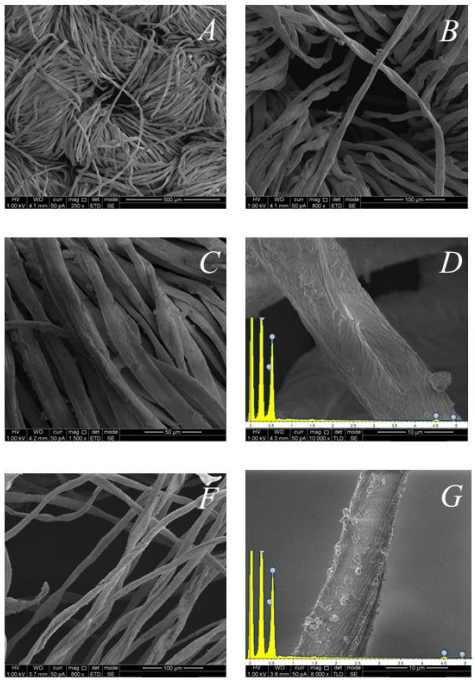

Fig. 1 – SEM images of (A, B) untreated fabric, (C-G) titania-nanosol prepared by method I(C,D) and II(F,G), and EDX analysis of TiO_2-modified fabrics (D,G).

X-ray diffraction and particle size distribution.

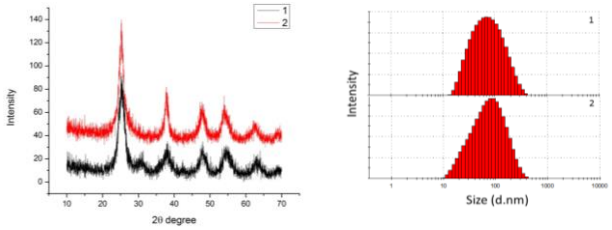

Fig. 2 – XRD figures of as-synthesized titania hydrosols prepared by method I (1) and II (2) and their hydrodynamic diameter distribution.

The XRD analysis results for crystalline titania hydrosols are shown in Fig. 2. The titania prepared using method I is characterized by the presence of crystalline anatase (*JCPDS*. No. 021-1272) and brookite (*JCPDS*. No. 29-1360) phases with respective average crystallite sizes of 4.7 and 3.9 nm. According to the data obtained, the produced titania represents anatase-brookite polymorph containing 58% of anatase and 42% of brookite. The sample prepared using method II is characterized by the presence of only one crystalline phase, anatase, with the average crystallite size of 4.9 nm.

Fig. 2 also shows the data on TiO_2 hydrosol nanoparticles hydrodynamic diameter size distribution. The hydrodynamic diameter of TiO_2 nanoparticles in sols is defined by the ionic strength of a medium. In this case it amounts to 70 nm for titania produced by method I, and 80 nm for that by method II, which testifies that agglomerates formed during hydrolysis are peptized by nitric or acetic acid to form a stable sol consisting of nanoparticles.

IR – Fourier spectroscopy

For estimating the interaction of BTCA with titania nanoparticles in a cotton fiber, the IR–Fourier spectroscopyresults (*Fig.3*) have been studied.

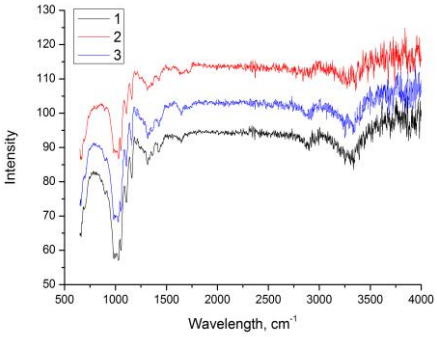

Fig. 3 – IR spectra of non-modified (1) cotton fiber and that modified (2,3) with titania hydrosol obtained using method I (2) and method II (3).

According to IR spectra, the modified cotton fibers (*Fig. 3* (*2,3*)) yield the peaks in the region of 1000–1300 cm^{-1}, characterizing the C–O–H bond stretching (1060 cm^{-1}) and the C–O–C bond vibration (1163 cm^{-1}) weakened as compared to the peaks for the sample 1–non-modified fiber. This fact occurs as a result of physical interaction of TiO_2 nanoparticles with the surface of a cotton fiber, which exercises the entrapping effect. The 1642cm^{-1} absorption band corresponding to the O=C bond vibration, is shifted as a result of the Ti–O–C bond vibration (from 1642 cm^{-1} to 1660 cm^{-1}). This fact reveals a strong interaction occurring on the interface between cotton fiber and titania nanoparticles in the Samples 2 and 3.

On the basis of data on studying morphology and IR spectroscopyresults, it is possible to assume that TiO_2 nanoparticles are cross-linked to the surface of a cotton fiber by forming transverse ester bonds with BTCA. The cellulose macromolecule is composed of glucose units linked together. The hydroxyl OH^- groups emerging from the macromolecular chain provide a strong cross-linkage to the functional groups of BTCA. An active five-membered cyclic anhydride is formed from 1,2,3,4-butanetetracarboxylic acid containing four functional carboxylic groups –COOH. The esterification reaction between cellulose and BTCA proceeds in three stages: at first there is a formation of cyclic anhydride by dehydration of two carboxylic groups, then the intermediate reacts with functional groups of cellulose to form transverse ester bonds. On the other hand, the two other free carboxylic groups of BTCA are linked to titania nanocrystalline sol by a strong electrostatic interaction. Sodium hypophosphite, in this case, acts as a catalyst of the reaction, increasing the rate of cross-linking the cellulose macromolecules to BTCA and TiO_2. It was revealed that NaH_2PO_2 weakens hydrogen

bonds between carboxylic acid functional groups in BTCA, promoting the accelerated formation of cyclic anhydride at low temperatures.

The process of TiO_2 interaction with cotton fibers also depends upon the concentration of acid used at an initial stage of producing titania nanocrystalline hydrosol. It may suggest that nitric and acetic acids operate as a catalyst of cellulose hydrolysis, leading to expansion of the chain of cellulose macromolecules and increasing the access of a cross-linking agent to functional groups of cellulose [11].

Self-cleaning properties and photocatalytic activity.

To study self-cleaning properties and photocatalytic activity of a fabric treated with titania nanosols, a Rhodamine B dye solution was prepared and the titania-nanosol-treated fabric was cut into small pieces and introduced into the dye solution. The solution was then exposed to a source of UV radiation for different periods of time as detailed in the Materials and Methods section. A Rhodamine B dye solution and Rhodamine B dye solution containing a control fabric (untreated) were also exposed to UV radiation at the same time (Fig. 5). The concentration of the dye in the solution was measured with a UV-Vis spectrophotometer. The evolution of the concentration of the dye in the solution as a function of the exposure time is shown in Figure 4.

The concentration of the dye in the solution containing the control fabric (Figure 4(1)) did not show any change with the UV radiation exposure time. This is also true for the dye solution (Figure 4(2)). When the nanosol-treated fabric is immersed in the dye solution and kept in the dark, the concentration of the dye did not change with time (Figure 4(3)). However, the concentration of the dye decreased when the solution containing nanosol-treated cotton fabric was exposed to UV radiation.For cotton fiber treated with titania sol prepared using method II, full decomposition of the dye was observed already in 45 minutes of radiation (Fig. 4(5)) resulting in a clear solution.

Thus, despite clear advantages of applying crystalline titania hydrosols for rendering self-cleaning properties of a cotton fiber, special attention must be paid to the type of acid applied as a peptizer of titania. Strong acids have negative effect resulting in fiber destruction. The present work suggests an optimum way to treat a cotton fiber with titania prepared in acetic acid at room temperature and using 1,2,3,4-butanetetracarboxylic acid as a cross-linking agent for rendering self-cleaning properties while retaining mechanical characteristics.

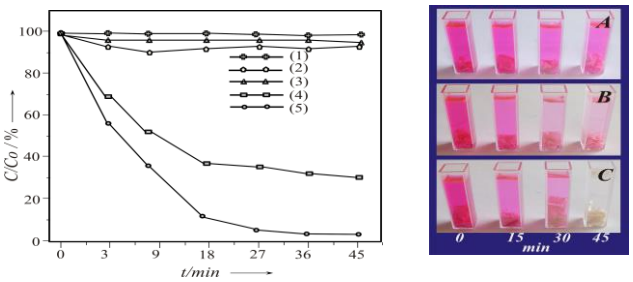

Fig. 4 – Left side: Decomposition of Rhodamine B dye: (1) Rhodamine B dye solution with no fabric; (2) Rhodamine B dye solution containing control white fabric; (3) Rhodamine B dye solution containing cotton fabric treated with titania nanosols and kept in the dark; (4) Rhodamine B dye solution containing cotton fabric treated with titania nanosols prepared by method I, (5) Rhodamine B dye solution containing cotton fabric treated with titania nanosols, prepared by method II and exposed to UV radiation for different periods of time. Right side: images of Rhodamine B dye decomposition in the water solution containing (A) control white fabric cotton; (B) cotton fabric treated with titania nanosols prepared by method I, (C) cotton fabric treated with titania nanosols prepared by method II.

In the present work, we have evaluated the effect of composition of crystalline titania hydrosols on mechanical and self-cleaning characteristics of a cotton fiber. 1,2,3,4-Butanetetracarboxylic acid has been applied as a cross-linking agent. The most promising sol for practical application among those selected is the titania hydrosol prepared in the medium of acetic acid. Content of anatase nanocrystallites allows to reach high photocatalytic activity, to avoid cellulose glycosidic bonds cleavage and, as a result, a loss in mechanical durability. Processed cotton fabrics exhibit almost full decomposition of the dye Rhodamine B already after 30 minutes of radiation.

AKNOWLEDGEMENTS

This work was supported by RFBR (№12-03-97538), the Ministry of Education and Science of the Russian Federation (No. 8632), and Russian President Grant for young PhD researcher MK-2229.2012.3.

REFERENCES

1. E.H. Lan, B.C. Dave, J.M. Fukuto, B. Dunn, J.I. Zink, J.S. Valentine, *J. Mater. Chem.* **9**, 45 (1999).
2. A. Rutenberg, V.V. Vinogradov, and D. Avnir, *J. Chem. Comm.* **49**, 5636 (2013).
3. K. Flora, J.D. Brennan, *Anal. Chem.* **70**, 4505 (1998).
4. E.H. Lan, B. Dunn, J.I. Zink, *Chem Mater.* **12**, 1874 (2000).
5. D.Q. Zhang, G.S. Li, X.F. Yang and J.C. Yu, *Chem. Commun.* **45**, 4381 (2009).
6. J.F. Moulder, W.F. Stickle, P.E. Sobol and K.D. Bomben, *Handbook of X-ray Photoelectron Spectroscopy*, (Ed. J. Chastain) (USA: Perkin-Elmer Corporation, 1992).
7. A.V. Vinogradov, V.V. Vinogradov, A.V. Agafonov, *Journal of Alloys and Compounds* **535**, 102 (2012).
8. X. Zhou, F. Peng, H. Wang, H. Yua, and Y. Fang, *Chem. Commun.* **48**, 600 (2012).
9. R. Su, R. Bechstein, J. Kibsgaard, R.T. Vang and F. Besenbacher, *J. Mater. Chem.* **22**, 23755 (2012).
10. N. Abidi, L. Cabrales, and E. Hequet *ACS Applied Materials & interfaces.* **1**, 2141 (2009).
11. P. Gupta, M. Bajpai, and S.K. Bajpai, *Journal of Macromolecular Science, Part A, Pure and Applied Chemistry.* **45**, 179 (2008).